Predicting Low-Field Visibility Loss from Local Opposite-Polarity Field Coupling

Matthew Crane
Independent Researcher
wxblayers@gmail.com

Abstract

Standard low-power optics treats visibility loss as a readout problem: the detector still records photon locations, but the measured hit pattern no longer separates cleanly into bright regions and dark regions.

This paper controls that readout explanation before the prediction is tested. First, a stable visible interference pattern is made. Then the dark-region background, detector noise, false counts, pixel scale, position uncertainty, and minimum distinguishable bright-dark difference are measured. That calibration sets the measured visibility limit of the tested setup.

After that calibration, detector sensitivity is part of the threshold test.

This paper predicts that the measurable interference zone shrinks as the beam-waist to opposite-polarity $\boxed{+}\boxed{-}$ coupling-event distance increases, until the setup reaches a measurable-visibility threshold.

The predicted measurable-visibility threshold distance is:

$$R_{\text{low}} = z_R\sqrt{\frac{P}{P_{\text{low}}} - 1}$$

1 Introduction

Standard low-power visibility explanations usually treat visibility loss as a detector signal-to-noise limit after the screen contrast becomes hard to measure. They do not begin by measuring the experiment's ***measured dark-region background-and-noise baseline*** and detector position-resolution scale as calibrated setup quantities.

This paper measures that baseline first. It also measures the detector position-resolution scale first. The threshold test then includes those calibrated setup quantities before testing the field-coupling prediction.

A shot-noise-limited detector-readout equation can be written as Eq. (1) [3,13,14]:

$$\mathrm{SNR} = \frac{\mathcal{R} P_{\mathrm{pixel}} \Delta t}{\sqrt{2e(\mathcal{R} P_{\mathrm{pixel}} + I_{\mathrm{dark}})\Delta t}} \tag{1}$$

Here **SNR** is the signal-to-noise ratio of a detector pixel, $\boldsymbol{\mathcal{R}}$ is detector responsivity, $\boldsymbol{P_{\mathbf{pixel}}}$ is the optical power reaching one detector pixel, $\boldsymbol{\Delta t}$ is exposure integration time, $\boldsymbol{e}$ is elementary charge, and $\boldsymbol{I_{\mathbf{dark}}}$ is detector dark current.

Eq. (1) is a detector readout equation. Its inputs are detector response, pixel power, exposure time, electron charge, and dark current [3,13,14]. Vacuum propagation, slit-boundary field structure, screen-position resolution, and the ***measured dark-region background-and-noise baseline*** are outside Eq. (1).

In that standard account, the screen detection pattern loses measurable visibility when the detector can no longer separate bright-region signal from the dark-region background and noise level [13–15]. In a vacuum setup, the screen still records photon-energy-event detections. The standard account therefore turns low-power visibility loss into a detector readout explanation.

This paper turns that readout explanation into measured setup data before the prediction is tested. The calibrated setup quantities are:

measured dark-region background-and-noise baseline

$\boldsymbol{x_{\mathbf{pixel}}}$

The ***measured dark-region background-and-noise baseline*** is the stable dark-region reading for the tested setup. It records the detector noise, dark current, background light, and false counts present in the experiment [13–15]. The quantity $\boldsymbol{x_{\mathbf{pixel}}}$ is the detector pixel size or minimum distinguishable screen-position distance [16,17].

These calibrated setup quantities are then built into the threshold test. The ***measured dark-region background-and-noise baseline*** sets the measured readout floor for the tested setup. The measured position-resolution quantity $\boldsymbol{x_{\mathbf{pixel}}}$ enters the calculation of $\boldsymbol{P_{\mathbf{low}}}$, the local organized coupling-event power cutoff for the tested setup.

This paper makes a separate field-coupling prediction. It treats the visible screen detection pattern as depending on the local organized coupling-event power available at the opposite-polarity $\boxed{+}\boxed{-}$ coupling event. That local organized coupling-event power is Eq. (2):

$$P_{\mathrm{coupling}}(r) = \frac{P}{1 + (r/z_R)^2} \tag{2}$$

The low-field visibility-loss condition is Eq. (3):

$$P_{\text{coupling}}(r) = P_{\text{low}} \tag{3}$$

Solving Eq. (3) with Eq. (2) gives Eq. (4):

$$R_{\text{low}} = z_R \sqrt{\frac{P}{P_{\text{low}}} - 1} \tag{4}$$

With sufficient spatial and intensity resolution, the measurable-interference zone is expected to shrink as $\boldsymbol{r}$ increases and local organized coupling-event power decreases. In this paper, visibility loss names the measurable-visibility threshold where the setup reaches its visibility cutoff.

A laser double-slit setup produces a visible screen detection pattern only when the propagating laser field disturbance maintains opposite-polarity $\boxed{+}\boxed{-}$ coupling events through the slit boundary and beyond it.

This paper treats visible interference as a field-coupling threshold. The central prediction is that visible interference fails when the opposite-polarity $\boxed{+}\boxed{-}$ coupling events become too weak to supply the required transverse photon-energy-event nudge.

The propagating laser field disturbance carries an oscillating electromagnetic structure. That oscillation forms a striped field-polarity structure made of $\boxed{+}$ field-polarity bands, $\boxed{-}$ field-polarity bands, and non-zero neutral divides.

The slit boundary shapes the incoming striped field-polarity structure into two shaped field paths. Beyond the slit boundary, the two shaped field paths form the crossing region. In the crossing region, a $\boxed{+}$ field-polarity band from one shaped field path can overlap a $\boxed{-}$ field-polarity band from the other shaped field path. When that overlap is opposite-polarity, it forms an opposite-polarity $\boxed{+}\boxed{-}$ coupling event.

The opposite-polarity $\boxed{+}\boxed{-}$ coupling event contains local coupling-event energy density. Counting that local coupling-event energy density over a wavelength-scale event volume gives coupling-event energy. Dividing the coupling-event energy by $\boldsymbol{c}$ gives coupling-event momentum.

The low-field visibility threshold occurs when the local organized coupling-event power reaches the setup-specific position-resolution cutoff.

As the beam-waist to opposite-polarity $\boxed{+}\boxed{-}$ coupling-event distance increases, the local organized coupling-event power decreases. The local coupling-event power-distance relation from Eq. (2) is:

$$P_{\text{coupling}}(r) = \frac{P}{1 + (r/z_R)^2} \tag{2}$$

where $\boldsymbol{P_{\text{coupling}}(r)}$ is the local organized coupling-event power at the opposite-polarity $\boxed{+}\boxed{-}$ coupling event distance $\boldsymbol{r}$, $\boldsymbol{P}$ is the laser power, and $\boldsymbol{z_R}$ is the Rayleigh range [8,9].

The low-field threshold condition from Eq. (3) is:

$$P_{\text{coupling}}(r) = P_{\text{low}} \tag{3}$$

where $\boldsymbol{P_{\text{low}}}$ is the non-zero local organized coupling-event power cutoff used for the visibility-loss condition. For a chosen setup, $\boldsymbol{P_{\text{low}}}$ is calibrated from the detector's smallest distinguishable screen-position distance, the slit-boundary to screen distance $\boldsymbol{L}$, the laser wavelength $\boldsymbol{\lambda}$, and the beam waist radius $\boldsymbol{w_0}$ [8–11,16,17].

Solving Eq. (3) with Eq. (2) gives the predicted visibility-loss distance in Eq. (4):

$$R_{\text{low}} = z_R \sqrt{\frac{P}{P_{\text{low}}} - 1} \tag{4}$$

Here $\boldsymbol{R_{\text{low}}}$ is the beam-waist to opposite-polarity $\boxed{+}\boxed{-}$ coupling-event distance where the local organized coupling-event power reaches $\boldsymbol{P_{\text{low}}}$.

The prediction is direct: increasing the beam-waist to opposite-polarity $\boxed{+}\boxed{-}$ coupling-event distance weakens coupling-event momentum, and the screen detection pattern loses measurable visibility near the predicted distance $\boldsymbol{R_{\text{low}}}$.

2 Oscillating Field Disturbance and Striped Field-Polarity Structure

The propagating laser field disturbance carries an oscillating electromagnetic structure from the laser source toward the slit boundary [5].

The oscillation forms alternating field-polarity bands within the propagating laser field disturbance. A $\boxed{+}$ field-polarity band names a local region where the electric-field orientation is in the positive field-polarity state of the oscillation. A $\boxed{-}$ field-polarity band names a local region where the electric-field orientation is in the negative field-polarity state of the oscillation. A non-zero neutral divide separates neighboring $\boxed{+}$ and $\boxed{-}$ field-polarity bands.

The striped field-polarity structure can be written schematically as:

$$\boxed{-}\ \boldsymbol{n}\ \boxed{+}$$

where $\boldsymbol{n}$ is the non-zero neutral divide between opposite field-polarity bands.

This striped field-polarity structure is the organized field structure that reaches the slit boundary. Locally, the slit boundary receives a $\boxed{+}$ field-polarity band, a non-zero neutral divide, and a neighboring $\boxed{-}$ field-polarity band as one ordered stripe unit.

The local stripe unit supplies the field-polarity structure that the slit boundary shapes into two shaped field paths. In the crossing region, a $\boxed{+}$ field-polarity band from one shaped field path and a neighboring $\boxed{-}$ field-polarity band from the other shaped field path can overlap as an opposite-polarity $\boxed{+}\boxed{-}$ coupling event.

3 Slit Boundary and Crossing-Region Coupling Event

The slit boundary receives the propagating laser field disturbance as a striped field-polarity structure.

The slit boundary shapes the incoming striped field-polarity structure into two shaped field paths. Each shaped field path carries a local stripe unit forward from the slit boundary: a $\boxed{+}$ field-polarity band, a non-zero neutral divide, and a neighboring $\boxed{-}$ field-polarity band.

Beyond the slit boundary, the two shaped field paths enter a crossing region. The crossing region is the local region where field-polarity bands from the two shaped field paths can overlap.

An opposite-polarity $\boxed{+}\boxed{-}$ coupling event occurs when a $\boxed{+}$ field-polarity band from one shaped field path overlaps a neighboring $\boxed{-}$ field-polarity band from the other shaped field path inside the crossing region.

The opposite-polarity $\boxed{+}\boxed{-}$ coupling event is the named local event where local coupling-event energy density is counted.

The physical chain through the crossing region is:

slit boundary
↓
two shaped field paths
↓
crossing region
↓
opposite-polarity $\boxed{+}\boxed{-}$ coupling event

The next section names the local coupling-event energy density inside the opposite-polarity $\boxed{+}\boxed{-}$ coupling event. That local coupling-event energy density is counted over a wavelength-scale event volume to obtain coupling-event energy. Dividing that coupling-event energy by $\boldsymbol{c}$ gives coupling-event momentum. The coupling-event momentum supplies the transverse photon-energy-event nudge associated with the visible screen detection pattern.

4 Local Coupling-Event Energy Density

The opposite-polarity $\boxed{+}\boxed{-}$ coupling event contains local coupling-event energy density at the crossing-region $\boxed{+}\boxed{-}$ overlap.

For a propagating electromagnetic field disturbance in vacuum, the local total field energy density is written as Eq. (5) [5,7]:

$$u = \epsilon_0 E^2 \tag{5}$$

Here $\boldsymbol{u}$ is the local electromagnetic field energy density, $\boldsymbol{\epsilon_0}$ is the vacuum permittivity, and $\boldsymbol{E}$ is the local electric-field strength of the propagating electromagnetic field disturbance.

The paper-specific quantity is the local coupling-event energy density inside the opposite-polarity $\boxed{+}\boxed{-}$ coupling event.

For the local $\boxed{+}\boxed{-}$ overlap, this paper names that same field energy density as the local coupling-event energy density in Eq. (6):

$$u_{+-} = \epsilon_0 E_{+-}^2 \tag{6}$$

Here $\boldsymbol{u}_{+-}$ is the local coupling-event energy density. $\boldsymbol{E}_{+-}$ is the electric-field strength of the opposite-polarity $\boxed{+}\boxed{-}$ overlap that forms the coupling event.

Eq. (6) names the energy density inside the local event where a $\boxed{+}$ field-polarity band from one shaped field path overlaps a neighboring $\boxed{-}$ field-polarity band from the other shaped field path.

This local coupling-event energy density is the physical quantity counted over a wavelength-scale event volume in the next section.

5 Coupling-Event Energy and Coupling-Event Momentum

The local coupling-event energy density $\boldsymbol{u}_{+-}$ is counted over a wavelength-scale event volume.

The wavelength-scale event volume is Eq. (7):

$$V_{\text{event}} = \lambda^3 \tag{7}$$

Here $\boldsymbol{V}_{\textbf{event}}$ is the local wavelength-scale event volume used to count coupling-event energy. The factor $\boldsymbol{\lambda\hat{}3}$ means one wavelength cubed.

The coupling-event energy is the local coupling-event energy density counted over the wavelength-scale event volume in Eq. (8):

$$E_{\text{coupling}} = u_{+-}\lambda^3 \tag{8}$$

Eq. (8) says that the opposite-polarity $\boxed{+}\boxed{-}$ coupling event contains coupling-event energy equal to its local coupling-event energy density multiplied by the wavelength-scale event volume.

Using the local coupling-event energy density from Eq. (6):

$$u_{+-} = \epsilon_0 E_{+-}^2 \tag{6}$$

Substituting Eq. (6) into Eq. (8) gives Eq. (9):

$$E_{\text{coupling}} = \epsilon_0 E_{+-}^2 \lambda^3 \tag{9}$$

Eq. (9) gives the coupling-event energy of the opposite-polarity $\boxed{+}\boxed{-}$ coupling event.

The coupling-event momentum is the coupling-event energy divided by the speed of light in Eq. (10) [2,4,6,7]:

$$p_{\text{coupling}} = \frac{E_{\text{coupling}}}{c} \tag{10}$$

Here $\boldsymbol{p_{\text{coupling}}}$ is the coupling-event momentum and $\boldsymbol{c}$ is the speed of light.

Substituting Eq. (9) into Eq. (10) gives Eq. (11):

$$p_{\text{coupling}} = \frac{\epsilon_0 E_{+-}^2 \lambda^3}{c} \tag{11}$$

Eq. (11) gives the coupling-event momentum carried by the opposite-polarity $\boxed{+}\boxed{-}$ coupling event.

The calculation chain in this section is:

local coupling-event energy density
↓
counted over wavelength-scale event volume
↓
coupling-event energy
↓
coupling-event momentum

The next section converts this field-density form into the measured-power form.

6 Measured-Power Form

The measured-power form expresses the same local coupling-event energy from Section 5 using laser power, beam area, and one wavelength of propagation.

The laser power available to one shaped field path is:

$$\boldsymbol{P/2}$$

Here $\boldsymbol{P}$ is the laser power and the factor $\boldsymbol{1/2}$ is the split factor for the two shaped field paths.

The Rayleigh range is Eq. (12) [8,9]:

$$z_R = \frac{\pi w_0^2}{\lambda} \tag{12}$$

Here $\boldsymbol{z_R}$ is the Rayleigh range, $\boldsymbol{w_0}$ is the beam waist radius, and $\boldsymbol{\lambda}$ is the laser wavelength.

At distance $\boldsymbol{r}$, the Gaussian beam area is Eq. (13) [8,9]:

$$A_{\text{beam}}(r) = \pi w_0^2 \left[1 + \left(\frac{r}{z_R}\right)^2\right] \tag{13}$$

Here $\boldsymbol{A_{\text{beam}}(r)}$ is the beam area at the opposite-polarity $\boxed{+}\boxed{-}$ coupling-event distance $\boldsymbol{r}$, $\boldsymbol{w_0}$ is the beam waist radius, and $\boldsymbol{z_R}$ is the Rayleigh range.

The measured-power form for the local coupling-event energy density uses the standard relation between electromagnetic intensity and field energy density in Eq. (14) [5]:

$$\epsilon_0 E_{+-}^2 = \frac{P/2}{cA_{\text{beam}}(r)} \tag{14}$$

Eq. (14) writes the local coupling-event energy density in measured-power form. The numerator $\boldsymbol{P/2}$ is the power carried by one shaped field path. The denominator $\boldsymbol{c\ A_{\text{beam}}(r)}$ converts power per beam area into local field energy density.

The wavelength-scale area of the local $\boxed{+}\boxed{-}$ overlap is Eq. (15):

$$A_{\text{overlap}} = \lambda^2 \tag{15}$$

Here $\boldsymbol{A_{\text{overlap}}}$ is the wavelength-scale local $\boxed{+}\boxed{-}$ overlap area and $\boldsymbol{\lambda\hat{}2}$ is one wavelength squared.

The coupling-event energy uses one wavelength of propagation through the local overlap area in Eq. (16):

$$E_{\text{coupling}}(r) = \left(\frac{P}{2}\right)\left(\frac{\lambda}{c}\right)\left[\frac{\lambda^2}{A_{\text{beam}}(r)}\right] \tag{16}$$

Eq. (16) is the measured-power form of the coupling-event energy. It counts the energy available to one shaped field path during one wavelength of propagation and multiplies that energy by the local overlap-area fraction:

$$\frac{\lambda^2}{A_{\text{beam}}(r)}$$

Substituting Eq. (13) into Eq. (16) gives:

$$E_{\text{coupling}}(r) = \left(\frac{P}{2}\right)\left(\frac{\lambda}{c}\right)\left[\frac{\lambda^2}{\pi w_0^2\left(1 + (r/z_R)^2\right)}\right]$$

Simplifying gives Eq. (17):

$$E_{\text{coupling}}(r) = \frac{P\lambda^3}{2\pi w_0^2 c\left(1 + (r/z_R)^2\right)} \tag{17}$$

Eq. (17) gives the coupling-event energy as a measured-power expression.

Dividing Eq. (17) by $\boldsymbol{c}$ gives coupling-event momentum in Eq. (18) [2,4,6,7]:

$$p_{\text{coupling}}(r) = \frac{E_{\text{coupling}}(r)}{c} \tag{18}$$

Substituting Eq. (17) into Eq. (18) gives Eq. (19):

$$p_{\text{coupling}}(r) = \frac{P\lambda^3}{2\pi w_0^2 c^2\left(1 + (r/z_R)^2\right)} \tag{19}$$

Eq. (19) gives the coupling-event momentum in measured-power form. As the distance $\boldsymbol{r}$ increases, $\boldsymbol{A_{\text{beam}}(r)}$ grows, the coupling-event energy decreases, and the coupling-event momentum decreases.

7 Low-Field Visibility Threshold

The ***measured dark-region background-and-noise baseline*** is established first. The stable dark-region reading gives the accepted baseline for false counts, background counts, and detector noise [13–15]. A valid threshold test must keep the ***measured dark-region background-and-noise baseline*** controlled.

For a given laser-slit-screen setup, the detector has a smallest screen-position distance that it can distinguish. That equipment sensitivity is set by the detector pixel size or position-resolution scale [16,17].

The slit-boundary to screen distance $\boldsymbol{L}$ converts that smallest distinguishable screen-position distance into the smallest transverse photon-energy-event nudge that the setup can resolve [10,11,16,17].

After the ***measured dark-region background-and-noise baseline*** is controlled, the remaining visibility limit is a position-resolution limit.

For a pixel detector, the minimum distinguishable screen-position distance can be taken as one pixel [16,17]. The slit-boundary to screen distance $\boldsymbol{L}$ converts that one-pixel screen displacement into the minimum transverse photon-energy-event nudge that the setup can resolve.

$\boldsymbol{P_{\mathbf{low}}}$ names the local organized coupling-event power required to maintain the smallest transverse photon-energy-event nudge that the setup can resolve. In this paper, $\boldsymbol{P_{\mathbf{low}}}$ is the non-zero local organized coupling-event power cutoff used for the visibility-loss condition. For a chosen setup, $\boldsymbol{P_{\mathbf{low}}}$ is calibrated from the detector's position-resolution limit, pixel size, and slit-boundary to screen distance $\boldsymbol{L}$.

The measured-power form in Eq. (19) shows that coupling-event momentum weakens as the beam-waist to opposite-polarity $\boxed{+}\boxed{-}$ coupling-event distance $\boldsymbol{r}$ increases.

Above $\boldsymbol{P_{\mathbf{low}}}$, the local organized coupling-event power is sufficient for the opposite-polarity $\boxed{+}\boxed{-}$ coupling event to maintain the measurable screen detection pattern.

At $\boldsymbol{P_{\mathbf{low}}}$, the local organized coupling-event power reaches the low-field visibility threshold.

For a chosen setup, $\boldsymbol{P_{\mathbf{low}}}$ can be calculated from the smallest screen-position distance that the detector can distinguish.

For a pixel detector, use the pixel size as the minimum distinguishable screen-position distance [16,17]:

$$\boldsymbol{x_{\mathbf{pixel}}}$$

The setup-specific cutoff is Eq. (20):

$$P_{\text{low}} = \frac{2\pi w_0^2 c^2 h x_{\text{pixel}}}{\lambda^4 L} \tag{20}$$

Here $\boldsymbol{w_0}$ is the beam waist radius, $\boldsymbol{c}$ is the speed of light, $\boldsymbol{h}$ is Planck's constant, $\boldsymbol{x_{\text{pixel}}}$ is the detector pixel size or minimum distinguishable screen-position distance, $\boldsymbol{\lambda}$ is the laser wavelength, and $\boldsymbol{L}$ is the slit-boundary to screen distance [1,2,8–11,16,17].

All quantities must be written in SI units:

$\boldsymbol{w_0}$ in meters

$\boldsymbol{x_{\text{pixel}}}$ in meters

$\boldsymbol{\lambda}$ in meters

$\boldsymbol{L}$ in meters

The result gives $\boldsymbol{P_{\text{low}}}$ in watts.

The physical meaning of this cutoff is resolvable parting of photon-energy-event detections on the screen. The transverse nudge supplies the momentum needed to separate photon-energy-event detections into distinguishable screen locations.

The local coupling-event power-distance relation from Eq. (2) is:

$$P_{\text{coupling}}(r) = \frac{P}{1 + (r/z_R)^2} \tag{2}$$

Here $\boldsymbol{P_{\text{coupling}}(r)}$ is the local organized coupling-event power at the opposite-polarity $\boxed{+}\boxed{-}$ coupling event distance $\boldsymbol{r}$, $\boldsymbol{P}$ is the laser power, and $\boldsymbol{z_R}$ is the Rayleigh range [8,9].

The low-field visibility threshold occurs when the local organized coupling-event power reaches $\boldsymbol{P_{\text{low}}}$ in Eq. (3):

$$P_{\text{coupling}}(r) = P_{\text{low}} \tag{3}$$

Substituting Eq. (2) into Eq. (3) gives:

$$\frac{P}{1 + (r/z_R)^2} = P_{\text{low}}$$

Solve for the threshold distance.

Start with:

$$\frac{P}{1+(r/z_R)^2} = P_{\text{low}}$$

Move the denominator:

$$P = P_{\text{low}}\left[1+(r/z_R)^2\right]$$

Divide by $\boldsymbol{P_{\text{low}}}$:

$$\frac{P}{P_{\text{low}}} = 1+(r/z_R)^2$$

Subtract $\boldsymbol{1}$:

$$\frac{P}{P_{\text{low}}} - 1 = (r/z_R)^2$$

Take the square root:

$$\sqrt{\frac{P}{P_{\text{low}}} - 1} = \frac{r}{z_R}$$

Multiplying by $\boldsymbol{z_R}$ gives Eq. (4):

$$R_{\text{low}} = z_R\sqrt{\frac{P}{P_{\text{low}}} - 1} \tag{4}$$

Here $\boldsymbol{R_{\text{low}}}$ is the beam-waist to opposite-polarity $\boxed{+}\boxed{-}$ coupling-event distance where the local organized coupling-event power reaches $\boldsymbol{P_{\text{low}}}$.

The physical chain for the low-field threshold is:

$$\begin{array}{c} \text{increasing } \boldsymbol{r} \\ \downarrow \\ \text{larger } \boldsymbol{A_{\mathbf{beam}}(r)} \\ \downarrow \\ \text{lower local organized coupling-event power} \\ \downarrow \\ \text{lower local coupling-event energy} \\ \downarrow \\ \text{lower coupling-event momentum} \\ \downarrow \\ \text{weaker transverse photon-energy-event nudge} \\ \downarrow \\ \text{loss of screen detection pattern visibility} \end{array}$$

The predicted visibility-loss distance is therefore Eq. (4):

$$R_{\text{low}} = z_R \sqrt{\frac{P}{P_{\text{low}}} - 1} \tag{4}$$

8 Numerical Reference Case

This section evaluates the predicted visibility-loss distance for a reference non-zero cutoff case.

Use the reference Rayleigh range [8,9]:

$$z_R = 1.57\,\text{m}$$

Use the reference non-zero visibility-loss cutoff:

$$P_{\text{low}} = 0.001\,\text{W}$$

The threshold-distance equation is Eq. (4):

$$R_{\text{low}} = z_R \sqrt{\frac{P}{P_{\text{low}}} - 1} \tag{4}$$

Substitute the reference values into Eq. (4):

$$R_{\text{low}} = 1.57 \sqrt{\frac{P}{0.001} - 1}$$

This substituted expression gives the predicted beam-waist to opposite-polarity $\boxed{+}\boxed{-}$ coupling-event distance where local organized coupling-event power reaches the non-zero visibility-loss cutoff $\boldsymbol{P_{\text{low}}}$.

For $\boldsymbol{P = 1\,\text{W}}$:

$$R_{\text{low}} = 1.57 \sqrt{\frac{1}{0.001} - 1}$$

$$R_{\text{low}} = 49.622929176\,\text{m}$$

At $\boldsymbol{P = 1\,\text{W}}$, the reference model predicts loss of screen detection pattern visibility near $\boldsymbol{R_{\text{low}} = 49.622929176\,\text{m}}$.

For $\boldsymbol{P = 100\,\text{W}}$:

$$R_{\text{low}} = 1.57 \sqrt{\frac{100}{0.001} - 1}$$

$$R_{\text{low}} = 496.475110252\,\text{m}$$

At $\boldsymbol{P = 100\,\text{W}}$, the reference model predicts loss of screen detection pattern visibility near $\boldsymbol{R_{\text{low}} = 496.475110252\,\text{m}}$.

For $\boldsymbol{P = 1000\,\mathrm{W}}$:

$$R_{\mathrm{low}} = 1.57\sqrt{\frac{1000}{0.001} - 1}$$

$$R_{\mathrm{low}} = 1569.999215000\,\mathrm{m}$$

At $\boldsymbol{P = 1000\,\mathrm{W}}$, the reference model predicts loss of screen detection pattern visibility near $\boldsymbol{R_{\mathrm{low}} = 1569.999215000\,\mathrm{m}}$.

Table 1. Reference low-field visibility-loss distances for $\boldsymbol{z_R = 1.57\,\mathrm{m}}$ and $\boldsymbol{P_{\mathrm{low}} = 0.001\,\mathrm{W}}$.

Laser power P	Substitution	Computed R_{low}
$\mathbf{1\,W}$	$\mathbf{1.57\sqrt{\frac{1}{0.001} - 1}}$	$\mathbf{49.622929176\,m}$
$\mathbf{100\,W}$	$\mathbf{1.57\sqrt{\frac{100}{0.001} - 1}}$	$\mathbf{496.475110252\,m}$
$\mathbf{1000\,W}$	$\mathbf{1.57\sqrt{\frac{1000}{0.001} - 1}}$	$\mathbf{1569.999215000\,m}$

The table shows the reference distance scale produced by Eq. (4) using the non-zero cutoff $\boldsymbol{P_{\mathrm{low}} = 0.001\,\mathrm{W}}$. Increasing laser power increases the beam-waist to opposite-polarity $\boxed{+}\boxed{-}$ coupling-event distance where the local organized coupling-event power reaches the same visibility-loss cutoff $\boldsymbol{P_{\mathrm{low}}}$.

9 Proposed Experiment

The proposed experiment measures whether the screen detection pattern loses visibility near the predicted low-field visibility-loss distance.

The controlled input quantities are:

$$\boldsymbol{P}$$
$$\boldsymbol{r}$$
$$\boldsymbol{w_0}$$
$$\boldsymbol{\lambda}$$
$$\boldsymbol{d}$$
$$\boldsymbol{L}$$

Here $\boldsymbol{P}$ is the laser power, $\boldsymbol{r}$ is the beam-waist to opposite-polarity $\boxed{+}\boxed{-}$ coupling-event distance, $\boldsymbol{w_0}$ is the beam waist radius, $\boldsymbol{\lambda}$ is the laser wavelength [8,9], $\boldsymbol{d}$ is the slit separation, and $\boldsymbol{L}$ is the slit-boundary to screen distance [10,11].

The calibrated setup quantities are:

$$\boldsymbol{x_{\mathrm{pixel}}}$$
measured dark-region background-and-noise baseline

Here $\boldsymbol{x_{\mathrm{pixel}}}$ is the detector pixel size or minimum distinguishable screen-position distance [16,17]. The ***measured dark-region background-and-noise baseline*** is the stable dark-region reading for the tested setup [13–15].

The derived setup cutoff is Eq. (20):

$$P_{\mathrm{low}} = \frac{2\pi w_0^2 c^2 h x_{\mathrm{pixel}}}{\lambda^4 L} \tag{20}$$

Here $\boldsymbol{P_{\mathrm{low}}}$ is the setup-specific local organized coupling-event power cutoff used for the visibility-loss condition.

The derived beam quantity is Eq. (12) [8,9]:

$$z_R = \frac{\pi w_0^2}{\lambda} \tag{12}$$

Here $\boldsymbol{z_R}$ is the Rayleigh range set by the beam waist radius and laser wavelength.

The measured output quantities are:

screen detection pattern
$$\boldsymbol{I_{\mathrm{max}}}$$
$$\boldsymbol{I_{\mathrm{min}}}$$
$$\boldsymbol{V}$$

Here $\boldsymbol{I_{\mathrm{max}}}$ is the bright-region intensity in the screen detection pattern, $\boldsymbol{I_{\mathrm{min}}}$ is the dark-region intensity in the screen detection pattern, and $\boldsymbol{V}$ is the measured fringe visibility.

The visibility measurement is Eq. (21) [12]:

$$V = \frac{I_{\mathrm{max}} - I_{\mathrm{min}}}{I_{\mathrm{max}} + I_{\mathrm{min}}} \tag{21}$$

Eq. (21) counts the contrast between a bright region and a neighboring dark region in the screen detection pattern.

For each tested setup, the predicted visibility-loss distance is Eq. (4):

$$R_{\text{low}} = z_R \sqrt{\frac{P}{P_{\text{low}}} - 1} \tag{4}$$

The experiment varies $\boldsymbol{r}$ through the predicted distance $\boldsymbol{R_{\text{low}}}$ and measures whether the screen detection pattern loses measurable visibility as the beam-waist to opposite-polarity $\boxed{+}\boxed{-}$ coupling-event distance crosses the low-field visibility threshold.

A supporting result is reproducible loss of measurable screen detection pattern visibility near the predicted distance $\boldsymbol{R_{\text{low}}}$.

The experiment should repeat the measurement for multiple values of $\boldsymbol{P}$, $\boldsymbol{w_0}$, and $\boldsymbol{\lambda}$. Changing $\boldsymbol{P}$, $\boldsymbol{w_0}$, or $\boldsymbol{\lambda}$ changes the computed value of $\boldsymbol{R_{\text{low}}}$. The prediction is that the measured visibility-loss distance should occur near the value of $\boldsymbol{R_{\text{low}}}$ computed from Eq. (4) for each tested setup.

The experiment should control beam alignment, slit-boundary distortion, slit heating, detector saturation, the ***measured dark-region background-and-noise baseline***, background light, air turbulence, dust, air, surface, or slit-edge scattering, laser power stability, laser coherence stability, mechanical vibration, beam clipping, and laser polarization stability [8–11,13–19]. Laser safety must be controlled before high-power or long-distance tests.

10 Expected Results, Discussion, and Limits

The expected supporting result is a reproducible loss of screen detection pattern visibility near the predicted distance in Eq. (4):

$$R_{\text{low}} = z_R \sqrt{\frac{P}{P_{\text{low}}} - 1} \tag{4}$$

This result is consistent with the field-coupling threshold if the screen detection pattern loses visibility near the predicted $\boldsymbol{R_{\text{low}}}$ for each tested setup.

The expected physical chain is:

increasing $\boldsymbol{r}$
$\downarrow$
larger $\boldsymbol{A_{beam}(r)}$
$\downarrow$
lower local organized coupling-event power
$\downarrow$
lower local coupling-event energy
$\downarrow$
lower coupling-event momentum
$\downarrow$
weaker transverse photon-energy-event nudge
$\downarrow$
loss of screen detection pattern visibility

A strong supporting result has three features.

First, the screen detection pattern remains visible while the local organized coupling-event power is above the setup-specific cutoff $\boldsymbol{P_{low}}$, where $\boldsymbol{P_{low}}$ is calculated from $\boldsymbol{x_{pixel}}$, $\boldsymbol{L}$, $\boldsymbol{\lambda}$, and $\boldsymbol{w_0}$ for the tested setup [8–11,16,17].

Second, the screen detection pattern loses measurable visibility as $\boldsymbol{r}$ crosses the predicted distance $\boldsymbol{R_{low}}$.

Third, changing $\boldsymbol{P}$, $\boldsymbol{w_0}$, or $\boldsymbol{\lambda}$ shifts the visibility-loss distance according to Eq. (4):

$$R_{\text{low}} = z_R \sqrt{\frac{P}{P_{\text{low}}} - 1} \tag{4}$$

A weakening result occurs if the screen detection pattern loses visibility far from the predicted distance $\boldsymbol{R_{low}}$, after $\boldsymbol{P}$, $\boldsymbol{w_0}$, $\boldsymbol{\lambda}$, and the setup conditions are measured and controlled.

The main experimental limits are:

beam alignment	***slit-boundary distortion***
slit heating	***detector saturation***
measured dark-region background-and-noise baseline	***background light***
air turbulence	***uncontrolled matter scattering in the beam path***
laser power stability	***laser coherence stability***
mechanical vibration	***beam clipping***
laser polarization stability	

Each visibility limit must be controlled because each limit can reduce measured fringe visibility without identifying the low-field coupling threshold [8–11,13–19]. Laser safety must be controlled before high-power or long-distance tests.

The threshold quantity $\boldsymbol{P_{\mathrm{low}}}$ names the non-zero local organized coupling-event power cutoff used for the visibility-loss condition. For a chosen setup, $\boldsymbol{P_{\mathrm{low}}}$ is calculated from $\boldsymbol{x_{\mathrm{pixel}}}$, $\boldsymbol{L}$, $\boldsymbol{\lambda}$, and $\boldsymbol{w_0}$ using Eq. (20). The ***measured dark-region background-and-noise baseline*** sets the measured readout floor for the tested setup.

The result of the proposed experiment is therefore judged by the measured relation between $\boldsymbol{r}$, $\boldsymbol{P}$, $\boldsymbol{w_0}$, $\boldsymbol{\lambda}$, $\boldsymbol{z_R}$, $\boldsymbol{P_{\mathrm{low}}}$, and screen detection pattern visibility.

11 Conclusion

This paper derives the low-field visibility threshold from the local opposite-polarity $\boxed{+}\boxed{-}$ coupling event.

The physical chain is:

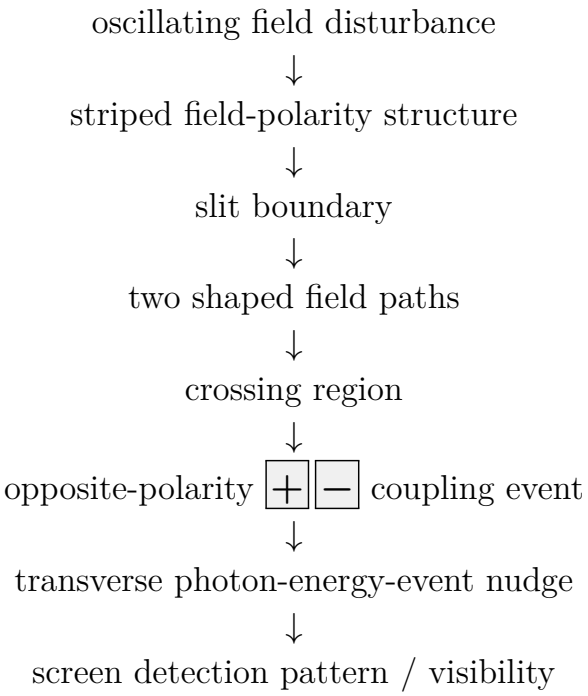

The coupling-event calculation is:

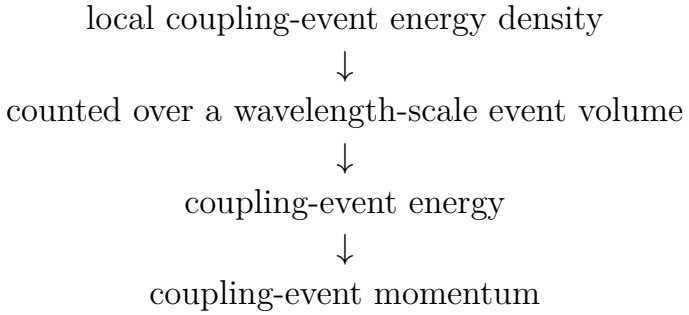

The opposite-polarity $\boxed{+}\boxed{-}$ coupling event contains local coupling-event energy density in Eq. (6):

$$u_{+-} = \epsilon_0 E_{+-}^2 \tag{6}$$

Counting that local coupling-event energy density over a wavelength-scale event volume gives coupling-event energy in Eq. (8):

$$E_{\text{coupling}} = u_{+-}\lambda^3 \tag{8}$$

Substituting Eq. (6) into Eq. (8) gives Eq. (9):

$$E_{\text{coupling}} = \epsilon_0 E_{+-}^2 \lambda^3 \tag{9}$$

Dividing Eq. (9) by $\boldsymbol{c}$ gives coupling-event momentum in Eq. (10) [2,4,6,7]:

$$p_{\text{coupling}} = \frac{E_{\text{coupling}}}{c} \tag{10}$$

Substituting Eq. (9) into Eq. (10) gives Eq. (11):

$$p_{\text{coupling}} = \frac{\epsilon_0 E_{+-}^2 \lambda^3}{c} \tag{11}$$

The measured-power form in Eq. (19) shows how the coupling-event momentum decreases as the beam-waist to opposite-polarity $\boxed{+}\boxed{-}$ coupling-event distance $\boldsymbol{r}$ increases:

$$p_{\text{coupling}}(r) = \frac{P\lambda^3}{2\pi w_0^2 c^2 \left(1 + (r/z_R)^2\right)} \tag{19}$$

The low-field visibility threshold is written as Eq. (3):

$$P_{\text{coupling}}(r) = P_{\text{low}} \tag{3}$$

with the local coupling-event power-distance relation from Eq. (2):

$$P_{\text{coupling}}(r) = \frac{P}{1 + (r/z_R)^2} \tag{2}$$

Here $\boldsymbol{P_{\text{low}}}$ is the setup-specific local organized coupling-event power cutoff calculated from $\boldsymbol{x_{\text{pixel}}}$, $\boldsymbol{L}$, $\boldsymbol{\lambda}$, and $\boldsymbol{w_0}$ using Eq. (20). The ***measured dark-region background-and-noise baseline*** sets the measured readout floor for the tested setup [13–15].

Solving Eq. (3) with Eq. (2) gives the predicted visibility-loss distance in Eq. (4):

$$R_{\text{low}} = z_R \sqrt{\frac{P}{P_{\text{low}}} - 1} \tag{4}$$

The central result is that the visibility-loss distance follows from the weakening of local opposite-polarity $\boxed{+}\boxed{-}$ coupling events as the local organized coupling-event power falls with distance. A supporting experiment measures whether the screen detection pattern loses measurable visibility near the predicted distance $\boldsymbol{R_{\text{low}}}$ for tested setups with controlled input quantities and calibrated setup quantities.

Symbol Table

Table 2. Symbols and units used in the low-field visibility-loss prediction.

Symbol	Meaning	Unit
P	laser power supplied to the setup	W
$P_{\mathrm{coupling}}(r)$	local organized coupling-event power at the opposite-polarity $\boxed{+}\boxed{-}$ coupling event distance r	W
P_{low}	setup-specific local organized coupling-event power cutoff for the measurable-visibility threshold	W
r	beam-waist to opposite-polarity $\boxed{+}\boxed{-}$ coupling-event distance	m
R_{low}	predicted measurable-visibility threshold distance where $P_{\mathrm{coupling}}(r)$ reaches P_{low}	m
w_0	beam waist radius	m
z_R	Rayleigh range	m
λ	laser wavelength	m
d	slit separation	m
L	slit-boundary to screen distance	m
x_{pixel}	detector pixel size or minimum distinguishable screen-position distance	m
$A_{\mathrm{beam}}(r)$	Gaussian beam area at distance r	m^2
A_{overlap}	wavelength-scale local $\boxed{+}\boxed{-}$ overlap area	m^2
V_{event}	wavelength-scale coupling-event volume	m^3
u	local electromagnetic field energy density	J/m^3
u_{+-}	local coupling-event energy density inside the opposite-polarity $\boxed{+}\boxed{-}$ coupling event	J/m^3
E	local electric-field strength of the propagating electromagnetic field disturbance	V/m
E_{+-}	electric-field strength of the opposite-polarity $\boxed{+}\boxed{-}$ overlap that forms the coupling event	V/m
E_{coupling}	coupling-event energy	J
p_{coupling}	coupling-event momentum	$kg\ m/s$
c	speed of light in vacuum	m/s
h	Planck's constant	$J\ s$
ϵ_0	vacuum permittivity	F/m
I_{max}	bright-region intensity in the screen detection pattern	W/m^2
I_{min}	dark-region intensity in the screen detection pattern	W/m^2
V	measured fringe visibility	dimensionless
SNR	signal-to-noise ratio of a detector pixel	dimensionless
$\mathcal{R}$	detector responsivity	A/W
P_{pixel}	optical power reaching one detector pixel	W
Δt	exposure integration time	s
e	elementary charge	C
I_{dark}	detector dark current	A

Appendix A. Units Check

This appendix checks the units of the main quantities used in the low-field visibility threshold derivation.

The local coupling-event energy density is:

$$u_{+-} = \epsilon_0 E_{+-}^2$$

The units are:

$$u_{+-} = \mathrm{J/m^3}$$

So $\boldsymbol{u_{+-}}$ is an energy density.

The wavelength-scale coupling-event volume is:

$$V_{\mathrm{event}} = \lambda^3$$

The units are:

$$V_{\mathrm{event}} = \mathrm{m^3}$$

The coupling-event energy is:

$$E_{\mathrm{coupling}} = u_{+-}\lambda^3$$

The units are:

$$E_{\mathrm{coupling}} = (\mathrm{J/m^3})(\mathrm{m^3})$$

$$E_{\mathrm{coupling}} = \mathrm{J}$$

So $\boldsymbol{E_{\mathrm{coupling}}}$ is an energy.

The coupling-event momentum is:

$$p_{\text{coupling}} = \frac{E_{\text{coupling}}}{c}$$

The units are:

$$p_{\text{coupling}} = \frac{\text{J}}{\text{m/s}}$$

$$p_{\text{coupling}} = \text{kg m/s}$$

So $\boldsymbol{p_{\text{coupling}}}$ is a momentum.

The Gaussian beam area is:

$$A_{\text{beam}}(r) = \pi w_0^2 \left[1 + \left(\frac{r}{z_R}\right)^2\right]$$

The units are:

$$A_{\text{beam}}(r) = \text{m}^2$$

because $\boldsymbol{w_0^2}$ has units $\boldsymbol{m\hat{}2}$, and $[\boldsymbol{1 + (r/z_R)^2}]$ is dimensionless.

The local organized coupling-event power is:

$$P_{\text{coupling}}(r) = \frac{P}{1 + (r/z_R)^2}$$

The units are:

$$P_{\text{coupling}}(r) = \text{W}$$

because $\boldsymbol{P}$ has units $\boldsymbol{W}$, and $[\boldsymbol{1 + (r/z_R)^2}]$ is dimensionless.

The threshold condition is:

$$P_{\text{coupling}}(r) = P_{\text{low}}$$

The units are:

$$\text{W} = \text{W}$$

So $\boldsymbol{P_{\text{low}}}$ is a setup-specific local organized coupling-event power cutoff.

The setup-specific cutoff is:

$$P_{\text{low}} = \frac{2\pi w_0^2 c^2 h x_{\text{pixel}}}{\lambda^4 L}$$

The units are:

$$P_{\text{low}} = \frac{(\text{m}^2)(\text{m}^2/\text{s}^2)(\text{J s})(\text{m})}{(\text{m}^4)(\text{m})}$$

$$P_{\text{low}} = \text{J/s}$$

$$P_{\text{low}} = \text{W}$$

So the setup-specific cutoff formula gives power.

The predicted measurable-visibility threshold distance is:

$$R_{\text{low}} = z_R \sqrt{\frac{P}{P_{\text{low}}} - 1}$$

The units are:

$$R_{\text{low}} = \text{m}\sqrt{\text{W}/\text{W} - 1}$$

$$R_{\text{low}} = \text{m}$$

So $\boldsymbol{R_{\text{low}}}$ is a distance.

The measured-power form of the coupling-event energy is:

$$E_{\text{coupling}}(r) = \frac{P\lambda^3}{2\pi w_0^2 c\,(1 + (r/z_R)^2)}$$

The units are:

$$E_{\text{coupling}}(r) = \frac{(\text{W})(\text{m}^3)}{(\text{m}^2)(\text{m/s})}$$

$$E_{\text{coupling}}(r) = \frac{(\text{J/s})(\text{m}^3)}{\text{m}^3/\text{s}}$$

$$E_{\text{coupling}}(r) = \text{J}$$

So the measured-power form also gives coupling-event energy.

The measured-power form of the coupling-event momentum is:

$$p_{\text{coupling}}(r) = \frac{P\lambda^3}{2\pi w_0^2 c^2 \left(1 + (r/z_R)^2\right)}$$

The units are:

$$p_{\text{coupling}}(r) = \frac{(\text{W})(\text{m}^3)}{(\text{m}^2)(\text{m}^2/\text{s}^2)}$$

$$p_{\text{coupling}}(r) = \frac{(\text{J/s})(\text{m}^3)}{\text{m}^4/\text{s}^2}$$

$$p_{\text{coupling}}(r) = \text{J s/m}$$

$$p_{\text{coupling}}(r) = \text{kg m/s}$$

So the measured-power form gives coupling-event momentum.

Appendix B. Equation Reference

Eq. (1) = detector readout / SNR equation Eq. (2) = local coupling-event power-distance relation Eq. (3) = low-field threshold condition Eq. (4) = predicted measurable-visibility threshold distance

Eq. (5) = standard electromagnetic field energy density Eq. (6) = paper-specific local $\boxed{+}\boxed{-}$ coupling-event energy density

Eq. (7) = wavelength-scale event volume Eq. (8) = coupling-event energy from local energy density Eq. (9) = coupling-event energy after substituting $\boldsymbol{u}_{+-}$ Eq. (10) = coupling-event momentum from $\boldsymbol{E_{\text{coupling}}/c}$ Eq. (11) = coupling-event momentum after substituting energy density

Eq. (12) = Rayleigh range Eq. (13) = Gaussian beam area Eq. (14) = measured-power form of local coupling-event energy density Eq. (15) = wavelength-scale overlap area Eq. (16) = measured-power coupling-event energy before simplification Eq. (17) = measured-power coupling-event energy after simplification Eq. (18) = measured-power coupling-event momentum from $\boldsymbol{E_{\text{coupling}}(r)/c}$ Eq. (19) = measured-power coupling-event momentum after substitution

Eq. (20) = setup-specific cutoff $\boldsymbol{P_{\text{low}}}$ Eq. (21) = measured fringe visibility

References

[1] NIST, "CODATA Value: Planck constant." https://physics.nist.gov/cgi-bin/cuu/Value?h

[2] NIST, "CODATA Value: speed of light in vacuum." https://physics.nist.gov/cgi-bin/cuu/Value?c

[3] NIST, "CODATA Value: elementary charge." https://physics.nist.gov/cgi-bin/cuu/Value?e

[4] OpenStax, *College Physics 2e*, "Photon Momentum." https://openstax.org/books/college-physics-2e/pages/29-4-photon-momentum

[5] OpenStax, *University Physics Volume 2*, "Energy Carried by Electromagnetic Waves." https://openstax.org/books/university-physics-volume-2/pages/16-3-energy-carried-by-electromagnetic-waves

[6] OpenStax, *University Physics Volume 2*, "Momentum and Radiation Pressure." https://openstax.org/books/university-physics-volume-2/pages/16-4-momentum-and-radiation-pressure

[7] R. P. Feynman, R. B. Leighton, and M. Sands, *The Feynman Lectures on Physics*, Vol. II, Ch. 27, "Field Energy and Field Momentum." https://www.feynmanlectures.caltech.edu/II_27.html

[8] R. Paschotta, "Gaussian Beams," *RP Photonics Encyclopedia*. https://www.rp-photonics.com/gaussian_beams.html

[9] R. Paschotta, "Rayleigh Length," *RP Photonics Encyclopedia*. https://www.rp-photonics.com/rayleigh_length.html

[10] OpenStax, *University Physics Volume 3*, "Young's Double-Slit Interference." https://openstax.org/books/university-physics-volume-3/pages/3-1-youngs-double-slit-interference

[11] OpenStax, *College Physics 2e*, "Young's Double Slit Experiment." https://openstax.org/books/college-physics-2e/pages/27-3-youngs-double-slit-experiment

[12] LibreTexts, "Fringe Visibility," *BSc Optics*. https://phys.libretexts.org/Bookshelves/Optics/BSc_Optics_%28Konijnenberg_Adam_and_Urbach%29/05%3A_Interference_and_coherence/5.10%3A_Fringe_Visibility

[13] Evident Scientific, "CCD Signal-to-Noise Ratio." https://evidentscientific.com/en/microscope-resource/knowledge-hub/digital-imaging/concepts/ccdsnr

[14] Hamamatsu, "What is dark noise?" https://camera.hamamatsu.com/jp/en/learn/technical_information/thechnical_guide/dark_noise.html

[15] Astropy, "Real dark current: noise and other artifacts," *CCD Reduction and Photometry Guide*. https://www.astropy.org/ccd-reduction-and-photometry-guide/v/dev/notebooks/03-02-Real-dark-current-noise-and-other-artifacts.html

[16] Edmund Optics, "Resolution." https://www.edmundoptics.com/knowledge-center/application-notes/imaging/resolution/

[17] Edmund Optics, "Camera Resolution for Improved Imaging System Performance." https://www.edmundoptics.com/knowledge-center/application-notes/imaging/camera-resolution-for-improved-imaging-system-performance/

[18] Ibsen Photonics, "Influence of polarization on fringe visibility." https://ibsen.com/resources/grating-resources/influence-of-polarization-on-fringe-visibility/

[19] J. C. Wyant, "Vibration insensitive interferometric optical testing." https://wp.optics.arizona.edu/jcwyant/wp-content/uploads/sites/13/2016/08/OFT-2004-OTuB2.pdf